energies

MDPI

Article

Exergetic, Energetic, and Quality Performance Evaluation of Paddy Drying in a Novel Industrial Multi-Field Synergistic Dryer

Bin Li, Changyou Li *, Tao Li, Zhiheng Zeng, Wenyan Ou and Chengjie Li

College of Engineering, South China Agricultural University, Guangzhou 510642, China
* Correspondence: lichyx@scau.edu.cn; Tel.: +86-20-85280817

Received: 25 October 2019; Accepted: 25 November 2019; Published: 2 December 2019

Abstract: The present work proposes a novel industrial multi-field synergistic dryer with a drying capacity of 3.45 t/h. The energy, exergy, and quality aspects of the drying process were studied. An energy–exergy methodology was employed to estimate the energetic and exergetic performance, heat loss characteristics and heat recovery behavior of the dryer. Additionally, the quality of the dried paddy seeds was evaluated by its crackle ratio, generation potential, and generation rate. The results showed that the overall energy and exergy efficiency ranged from 13.26% to 56.63% and 39.03% to 60.23%, respectively. The improvement potential rates of the whole system varied from the lowest 8.49 kW to the highest 15.83 kW and respectively accounted for 15.81–29.48% of the total exergy input, indicating that the performance of the dryer is acceptable. The total recovered radiant energy and radiant exergy recover rate were respectively ascertained to be 237.64 MJ and 0.26 kW. As for the quality aspect, the generation potential and generation rate of the dried paddy seeds respectively ranged from 75% to 90% and 69% to 88% while the crackle ratio of the paddy seeds was 1%, which indicated that the quality performance of the dried seed is of economic viability.

Keywords: exergy; energy; drying; paddy; industrial; quality

1. Introduction

Drying (also dehydration or dewatering) is a typical irreversible thermodynamic process which is affected not only by external constraints (e.g., the drying process and ambient conditions), but also by the inherent properties of materials, the thermodynamic mechanism of the drying process, and the dynamic irreversible characteristics of the interactions [1]. Revealing the energy structure, energy transfer, and conversion mechanism in the drying process from both internal and external aspects is one of effective methods to maximize overall energy efficiency and reduce energy loss in the drying process. As a high-energy consumption operation in industrial production, drying consumes about 10–25% of the national energy each year [2–4], and energy is an essential factor in overall efforts to achieve sustainable development. Therefore, it is of great significance to explore the drying theory and energy-saving technologies for the drying industry.

Paddy drying is a highly energy-intensive operation and sensitive to the quality of the dried product. In the last few decades, many researchers have carried out a great deal of research on the energy consumption and the quality investigation of paddy drying [5–11], however, seldom studies about industrial-scale paddy drying technologies have been reported. In order to find an energy-saving and high-quality industrial paddy drying technology, researchers have conducted some studies on the energy-saving or high-quality drying technologies. For example, Sarker et al., reported an industrial fluidized bed dryer in 2015 [12] and found that the energy efficiency of the drying process ranged from 5.24% to 13.92% and recommended that the energy efficiency should be further improved by recycling

the waste energy in the exhaust air and enhancing the insulation of the dryer body. Sarker et al. investigated the impact of drying temperature and air flow on energy consumption and the quality of rice (head rice yield and whiteness of rice) during paddy drying in an industrial inclined bed dryer [13]. Considering the recommendations mentioned above and based on our previous works, the present work proposed a general-purpose industrial multi-field synergistic dryer equipped with a waste heat recovery equipment. Moreover, in the drying process, the energy waste mainly includes the energy loss to surroundings and energy destroyed. It is necessary to reveal where and how much the energy is lost and destroyed in the drying system. The energy–exergy methodology can reveal where and by how much it is possible to design more efficient thermal systems by reducing the sources of existing inefficiencies [14].

A large number of studies about energy and exergy analysis in drying process [15–20] have been reported based on the quantity conservation of the energy consumption (First law of thermodynamics). For instance, Aviara et al. investigated the performance of the native cassava starch drying in a tray dryer by using energy–exergy methodology and the results showed that exergy efficiency increased with increase in both drying air temperature and energy utilization and was lower than energy efficiency [21]. Aktaş et al. worked on the minimized energy consumption and maximized exergetic efficiency of grated carrot drying [22]. Hazervazifeh et al. studied and compared the energy consumption, thermal efficiency, and the drying time of apple slices drying in a novel hybridized dryer under different drying conditions [23]. From the literature review, it can be seen that the exergy–energy methodology was widely used in drying process. Although there are a large amount of studies about exergy and energy performance for agro-product drying have been reported, few works have appeared on exergy, energy, and quality aspects performance for industrial paddy drying. Furthermore, though many researchers have studied industrial paddy drying technologies, there are still few reports about the multi-field synergistic drying. The present work proposed a novel industrial multi-field synergistic drying system which has the advantages of far-infrared drying, flash drying, and hot air drying. Based on the first and second law of thermodynamics, the present work focuses on energetic and exergetic performance, energy recovery performance and the heat loss characteristics of paddy drying in a novel industrial multi-field synergistic dryer. In addition, the quality aspect of the dried rice was also investigated so as to increase economic benefit and improve the energy utilization level in the rice processing industry.

2. Materials and Methods

2.1. Materials

The freshly paddy (Xiangzao Chan 45#), as shown in Figure 1, was harvested from a local farmer at Leizhou Guangdong Province, China. The average initial moisture content is 25.06% (w.b.). The impurity content is less than 5% and the content of long stems (length ≤ 50 mm) is less than 1%.

Figure 1. The freshly paddy sample for the experiment.

2.2. Equipment Description and the Working Principle

The schematic diagram of the dryer is shown in Figure 2. As shown in the diagram, the multi-field synergistic drying chamber mainly consists of three sections including far-infrared section (I), flash drying section (II), reverse mixed drying section (III), and the controller set the power for the entire system. In the drying process, the paddy is lifted by the conveyor and falls into the dryer body from the inlet. After the dryer is full, the induced draft fan, the under-belt conveyor, the hoist and the discharging device are sequentially opened. Then the seeds sequentially flow through the far-infrared section (I), flash drying section (II), exhaust angle box, the reverse mixed drying section (III), the inlet angle box, and the grain discharge section, grain discharge device, conveyor and then to the hoist. The temperature of inlet air ($T_{a,in}$), outlet air ($T_{a,out}$), ambient (T_∞), radiator (T_r), and the humidity of inlet air ($H_{a,in}$), outlet air ($H_{a,out}$), and the ambient (H_∞) were monitored by the corresponding sensors connected with data acquisition system and the corresponding designed values of the temperatures are tabulated in Table 1. The moisture content and temperature of the outlet paddy were measured by a self-developed online moisture meter (capacitance mode) which were pre-calibrated by using the 105 °C constant weight methodology. The details of the experimental instruments are listed in Table 2.

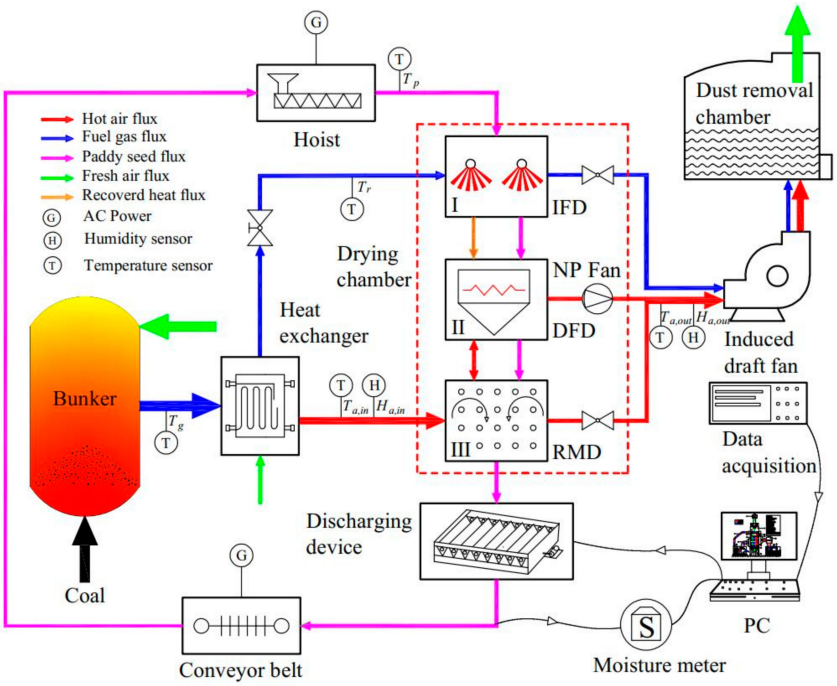

Figure 2. The schematic diagram of the multi-field synergistic drying system.

Table 1. The designed values of the related parameters adopted in the work.

Parameters	Designed Values	Considerations
Inlet air temperature ($T_{a,in}$)	70 °C	Specific high initial moisture content
Outlet air temperature ($T_{a,out}$)	30 °C	To decrease the heat loss in outlet air
Outlet paddy temperature ($T_{p,out}$)	30 °C	To decrease the heat loss in outlet paddy
Flue gas temperature (T_g)	400 °C	Empirical
Radiator temperature (T_r)	90 °C	The paddy seed get the optimal absorption wavelength (9 μm) when T_r is 90 °C

Note: The ambient conditions are considered to be constant at 28.5 °C and 101.325 kPa.

Table 2. The details of the experimental instruments.

Devices	Model	Measurement Range	Precision	Uncertainly
Thermal resistance	PT100	−200–450 °C	±0.1 °C	±0.133 °C
Anemometer	DT-8893	0.001–45 m/s	0.01 m/s	0.0234 m/s
Temperature and humidity sensors	AM2301	0–100%/−40–80 °C	±3%/±0.5 °C	±3.102%/±0.534 °C
Data acquisition system	Self-developed	-	-	-
Moisture meter	Self-developed	10–40%	±0.5%	±0.5136%

The scene graph of the multi-field synergistic dryer is shown in Figure 3. In the drying process, the fresh paddy is lifted by the hoist and then flows through the far-infrared section (IFD) which mainly consists of four tubular infrared radiators. In this section, the thermal energy in high temperature flue gas is converted into radiant energy by the radiators. Since the far-infrared radiators are inserted in the dryer and surrounded by flowing seeds, the view factor of the radiator against the seeds in the dryer is equal to 1, that is, the radiant energy generated by the appearance of the radiator is totally absorbed by the seeds. Moreover, the radiant energy supplement the internal energy of the seeds and improve the tissue function of the paddy seeds. The paddy seeds then flow through the depressurized flash drying section (DFD) under the function of gravity. Since the moisture content of grain is above 25% (w.b.), the binding energy between water molecules and ingredient is negligible, the dehydration process can be regarded as water evaporation in the free state [24]. Therefore, the high-humidity grain dehydrates rapidly in the low-pressure medium and further leading to the temperature of the grain surface decreases rapidly. The result is that the surface temperature of the grain is rapidly decreased and form a forward temperature gradient (the direction of heat and mass transfer are same), which not only ensures the grain drying temperature is not over-limit, but also improves the moisture activity inside the grain and enhances the driving force in drying. After far-infrared and flash drying, the moisture content of the grain is greatly reduced and then flows through the RMD (section III), in the process, the longitudinal flow velocity and the lateral displacement of the grain are continuously changed under the diversion of the variable cross-section box, which not only ensures the uniformity of drying but also increases the drying rate.

Figure 3. The scene graph of the multi-field synergistic dryer.

2.3. Energy Performance

In the present work, the general used mass and energy balance equations (Equations (1) and (2)) [25,26] were adopted to analyze the energetic performance of the drying system which is assumed to be at a steady state and steady flow process, the equations are listed as follows:

$$\sum \dot{m}_{in} = \sum \dot{m}_{out} \tag{1}$$

$$\sum \dot{E}_{in} = \sum \dot{E}_{out} \tag{2}$$

or:

$$\sum \dot{m}_{in} \dot{h} = \sum \dot{m}_{out} \dot{h} \tag{3}$$

With all energy terms, the Equation (2) can be expressed as Equation (4):

$$\sum \dot{Q} + \sum \dot{m}_{in} \dot{h}_{in} = \sum \dot{W} + \sum \dot{P} + \sum \dot{m}_{out} \dot{h}_{out} \tag{4}$$

The overall energy efficiency (η_{en}) was defined as the ratio of effective energy for the unit drying operation to the total energy consumption of the system, of which the effective energy consisted of energy for evaporation (E_{evap}), and work for transmitting ($W_{conveyor}$) and lifting (W_{hoist}) the paddy seeds, while the total energy consumption mainly consisted of the fuel consumption (Q_{fuel}), electrical energy consumption of the fan (P_{fan}), electrical energy consumption at the conveyor ($P_{conveyor}$), electrical energy consumption at the hoist (P_{hoist}), and energy consumption in other parts (P_{mix}), as shown in Figure 2. Hence, the overall energy efficiency of the whole multi-field drying system ($\eta_{en,w}$) and energy efficiency of the drying chamber ($\eta_{en,c}$) can be respectively computed by Equations (5) and (6):

$$\eta_{en,w} = \frac{\dot{E}_{evap} + \dot{W}_{hoist} + \dot{W}_{conveyor}}{\dot{Q}_{fuel} + \dot{P}_{fan} + \dot{P}_{nfan} + \dot{P}_{hoist} + \dot{P}_{conveyor} + \dot{P}_{mix}} \tag{5}$$

$$\eta_{en,c} = \frac{\dot{E}_{evap}}{\dot{E}_{a,in} + \dot{P}_{fan} + \dot{E}_{FIR}} \tag{6}$$

2.4. Exergy Analysis

The general exergy balance equation based on the second law of thermodynamics was adopted to analyze the exergetic performance of the drying chamber [26]. The developed equation in rate form is expressed as:

$$\sum \dot{E}x_{in} - \sum \dot{E}x_{out} = \sum \dot{E}x_{des} \tag{7}$$

Equation (7) can be rewritten as Equations (8) and (9):

Drying chamber:

$$\dot{E}x_{a,in} + \dot{E}x_{p,in} + \dot{E}x_{FIR} + \dot{E}x_{DFD} - \dot{E}x_{a,out} - \dot{E}x_{p,out} + \dot{E}x_{evap} - \dot{E}x_{loss} = \dot{E}x_{des} \tag{8}$$

Whole system:

$$\dot{E}x_{fuel} + \dot{W}_{hoist} + \dot{W}_{conveyor} + \dot{P}_{fan} + \dot{P}_{nfan} + \dot{P}_{mix} - \dot{E}x_{a,out} - \dot{E}x_{p,out} - \dot{E}x_{evap} - \dot{E}x_{loss} = \dot{E}x_{des} \tag{8a}$$

where the effective work done by hoist and conveyor can be expressed as follows [27]:

$$\dot{W}_{conveyor} = \frac{m_{l,c} v^2}{2} \tag{9}$$

$$\dot{W}_{hoist} = \frac{m_{l,h}v^2}{2} + m_{l,h}gv \tag{10}$$

According to some open literature [17,26,28], the exergy model of mixture can be expressed as Equation (11):

$$\dot{Ex} = (h - h_\infty) - T_\infty(s - s_\infty) \tag{11}$$

$$h - h_\infty = c_p(T - T_\infty) \tag{11a}$$

$$s - s_\infty = c_p \ln\left(\frac{T}{T_\infty}\right) - R\ln\left(\frac{P}{P_\infty}\right) \tag{11b}$$

Based on Equation (11), the specific exergy of the inlet and outlet paddy seeds ($\dot{Exp}$) can be calculated followed by Equation (12). Additionally, according to some open literature [17,28–30], the specific exergy of the mixture of dry air and water vapor can be calculated followed by Equation (13), so the mixed air flux entering and leaving the drying chamber ($\dot{Ex}_a$) in this work can be also calculated according to Equation (13):

$$\dot{Ex}_p = C_p\dot{m}_p\left[(T_p - T_\infty) - T_\infty \ln\left(\frac{T_p}{T_\infty}\right)\right] \tag{12}$$

$$\dot{Ex}_a = \dot{m}_a\left\{\begin{array}{c}(C_a + \omega C_v)(T_a - T_\infty) - T_\infty\left[(C_a + \omega C_v)\ln\left(\frac{T_a}{T_\infty}\right) - (R_a + \omega R_v)\ln\left(\frac{P_a}{P_\infty}\right)\right] \\ +T_\infty\left[(R_a + \omega R_v)\ln\left(\frac{1+1.6078\omega_\infty}{1+1.6078\omega}\right) + 1.6078\omega R_a \ln\left(\frac{\omega}{\omega_\infty}\right)\right]\end{array}\right\} \tag{13}$$

The exergy loss rate ($\dot{Ex}_{loss}$) introduced by the heat loss of the drying chamber ($\dot{Q}_{loss}$) can be computed by Equation (14) [17]:

$$\dot{Ex}_{loss} = \left(1 - \frac{T_\infty}{T_c}\right)\sum \dot{Q}_{loss} \tag{14}$$

The heat loss of the dying chamber are mainly consisted of three aspects which are the heat loss in the outlet air ($Q_{a,out}$), the heat loss in outlet paddy seeds ($Q_{p,out}$) and the heat loss in the chamber wall (Q_{wall}). Hence, the heat loss of the drying chamber can be calculated followed by the Equation (15) [24]:

$$\sum \dot{Q}_{loss} = \dot{Q}_{a,out} + \dot{Q}_{p,out} + \dot{Q}_{wall} \tag{15}$$

$$\dot{Q}_{wall} = 1.3A_s\frac{T_{wall} - T_{\infty,\min}}{\frac{\delta}{\gamma} + \frac{1}{1.163(6+0.5v_\infty)}} \tag{15a}$$

$$\dot{Q}_{p,out} = C_p\dot{m}_p(T_{p,out} - T_\infty) \tag{15b}$$

$$\dot{Q}_{a,out} = \dot{m}_{a,out}(h_{a,out} - h_\infty) \tag{15c}$$

The mass flow rate of the outlet dry air ($\dot{m}_{a,out}$) can be determined by Equation (16) [17]:

$$\dot{m}_{a,out} = \rho_{da}.V.S \tag{16}$$

where V is the velocity of the outlet air; S is the area of the outlet pipeline; ρ_{da} is the density of the dry air which can be determined by Equation (17) [19]:

$$\rho_{da} = \frac{101.325}{0.287T_{abs}} \tag{17}$$

The enthalpies of the outlet drying air (ha,out) can be computed followed by Equation (18) [17]:

$$h_{a,out} = (C_a + \omega C_v)(T_{a,out} - T_\infty) + \omega h_{fg} \tag{18}$$

The exergy rate ($\dot{E}x_{evap}$) used for evaporating the moisture from the paddy seeds is defined by Equation (19) [26]:

$$\dot{E}x_{evap} = \left(1 - \frac{T_\infty}{T_p}\right)\dot{Q}_{evap} \tag{19}$$

$$\dot{Q}_{evap} = \dot{m}_{Dehydrated\ water} h_{fg} \tag{19a}$$

In the far-infrared drying section, the radiation wavelength (λ) can be computed based on the Wien Displacement Law [31], and the recovered radiant energy and exergy by the radiators can be respectively computed followed by Equations (21) and (22) [32]:

$$\lambda \cdot T = 2897.6um \cdot K \tag{20}$$

$$\dot{E}_{FIR} = \sigma \varepsilon_r T_r^4 \tag{21}$$

$$\dot{E}x_{FIR} = \sigma T_r^4 \left(\varepsilon_r + \frac{1}{3}\left(\frac{T_\infty}{T_r}\right)^4 - \frac{4}{3}\varepsilon_r^{-0.75}\left(\frac{T_\infty}{T_r}\right)\right) \tag{22}$$

In the depressurized flash drying section, the preheated grain with different moisture content evaporated rapidly under a negative pressure (20 Kpa) due to the relation of linear change of boiling point and pressure of water. Flash drying can improve the tissue function of the seed and improve the drying quality including germination rates and crackle ratio. Owning to the energy quality coefficient of electric energy is equal to 1, the exergy inputted into the drying chamber by the negative-pressure air fan can be calculated followed by Equation (23):

$$\dot{E}x_{DFD} = \dot{W}_{fan} \tag{23}$$

The overall exergy efficiency ($\eta_{ex,w}$), exergy efficiency of the drying chamber ($\eta_{ex,c}$), specific energy consumption (SEC), exergetic improvement potential rate ($\dot{IP}$), and exergetic sustainability index (SI) were adopted to evaluate the exergy performance of the drying system, and the indices were determined as follows, respectively [17,19,28]:

$$\eta_{ex,ch} = \frac{\dot{E}x_{evap}}{\dot{E}x_{a,in} + \dot{E}x_{FIR} + \dot{E}x_{DFD}} \tag{24}$$

$$\eta_{ex,w} = \frac{\dot{E}x_{evap} + \dot{W}_{hoist} + \dot{W}_{conveyor}}{\dot{E}x_{a,in} + \dot{E}x_{FIR} + \dot{E}x_{DFD} + \dot{P}_{hoist} + \dot{P}_{conveyor} + \dot{P}_{mix}} \tag{25}$$

$$SEC = \frac{E_{fuel} + E_{fan} + E_{nfan} + E_{hoist} + E_{conveyor} + E_{mix}}{m_{Dehydrated\ water}} \tag{26}$$

$$\dot{IP} = (1 - \eta_{ex})\left(\dot{E}x_{in} - \dot{E}x_{out}\right) \tag{27}$$

$$SI = \frac{1}{(1 - \eta_{ex})} \tag{28}$$

In the present work, the dead state was considered to be the conditions of the ambient at which the temperature, pressure, air velocity, and absolute humidity were 28.5 °C, 101.325 kPa, 0.2 m·s^{-1}, and 0.018 kg water·kg^{-1} dry air, respectively. The latent heat of condensation was neglected in the present work. Additionally, the thermodynamic values and related equations used for calculating the indices mentioned above are tabulated in the Table 3, the nomenclature of the symbols adopted in this work are tabulated in the Nomenclature.

Table 3. Ambient conditions, thermodynamic values, and related equations used in the present work.

Parameters Name	Value/Equation	Unit	Reference
R_a	0.287	$kJ \cdot kg^{-1} \cdot K^{-1}$	[19]
R_v	0.462	$kJ \cdot mol^{-1} \cdot K^{-1}$	
σ	5.67×10^{-8}	$W \cdot m^{-2} \cdot K^{-4}$	[32]
ϵ_r	0.9	-	
A_r	8.3	m^2	
δ	0.02	m	
γ	1.0	$W \cdot m^{-1} \cdot K^{-1}$	
S	18.1	$m \cdot s^{-1}$	
A	0.126	m^2	
$\dot{m}_p$	17.223	$kg \cdot s^{-1}$	
C_p	$C_p = 1.12 + 0.045M$	$kJ \cdot kg^{-1} \cdot K^{-1}$	[33]
h_{fg}	$h_{fg} = \left(7.33 \times 10^{12} - 1.60 \times 10^7 T_k^2\right)^{0.5}$ $338.72 \le T_k(K) \le 553.16$	$kJ \cdot kg^{-1}$	[34]
C_v	$C_v = 1.883 - \left(1.6737 \times 10^{-4} T\right) + \left(8.4386 \times 10^{-7} T^2\right) - \left(2.6966 \times 10^{-10} T^3\right)$	$kJ \cdot kg^{-1} \cdot K^{-1}$	[28]
C_a	$C_a = 1.04841 - \left(3.83719 \times 10^{-4} T\right) + \left(9.45378 \times 10^{-7} T^2\right) - \left(5.49031 \times 10^{-10} T^3\right) + \left(7.9298 \times 10^{-14} T^4\right)$	$kJ \cdot kg^{-1} \cdot K^{-1}$	
Radiator size	$D_0 = 0.22$; $D_i = 0.2$; $L = 3$	m	

2.5. Drying Kinetics and Quality Performance

In this work, the wet basis moisture content (M) and the drying rate (DR) of the paddy can be calculated by Equations (29) and (30), respectively [35,36]:

$$M = \frac{m_i - m_d}{m_i} \times 100\% \tag{29}$$

$$DR = \frac{M_{t+\Delta t} - M_t}{M_{t+\Delta t}} \times 100\% \tag{30}$$

The quality performance of the dried paddy seeds in this work was evaluated by the germination rates (GR) and crackle ratio (CR), of which GR was measured followed by the method reported by Li (2004) [37] while the CR was measured under a burst waist lamp by Equations (31) and (32), respectively:

$$\eta_{GR} = \frac{n_g}{N} \times 100\% \tag{31}$$

$$\eta_{CR} = \frac{(w_1 + w_2)}{w} \times 100\% \tag{32}$$

2.6. Uncertainty Analysis

Uncertainty analysis is a commonly used effective method for evaluating the experimental results. In the present study, the experimental errors and uncertainties mainly arose from the convective dryer, instrument accuracy, ambient conditions, observation, and the test planning. Uncertainties of the experimental in this work were ascertained by Equations (33) and (34) [38]:

$$R = \sum_{i=1}^{r} R_i / r \tag{33}$$

$$u = \left(\frac{1}{r-1}\right) \sum_{i=1}^{r} (R_i - R) \tag{34}$$

3. Results and Discussions

3.1. Drying Performance of the Dryer

In the present work, the exergetic, thermal, and drying performance of an industrial multi-field drying system were investigated, respectively. The actual air supply weight of the system is 9556.645 kg/h and hold up as 31,000 kg during the drying unit. The initial moisture content of the grain for the experiment is 25.06% w.b. In the drying process, the moisture content of the grain, the temperature of inlet air, outlet air, ambient, radiator, chamber wall and the grain, the relative humidity of the inlet air and outlet air were measured at 30 min intervals, respectively. The drying performance of the dryer was evaluated by the drying kinetics, crackle ratio and generation ratio of the dried product, the results are shown in Figures 4–6, respectively.

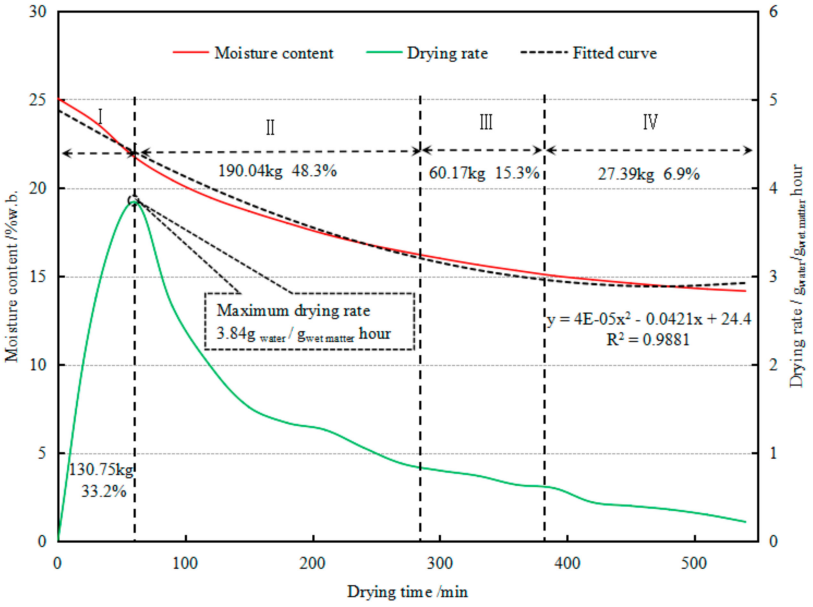

Figure 4. The kinetics curves of the paddy drying.

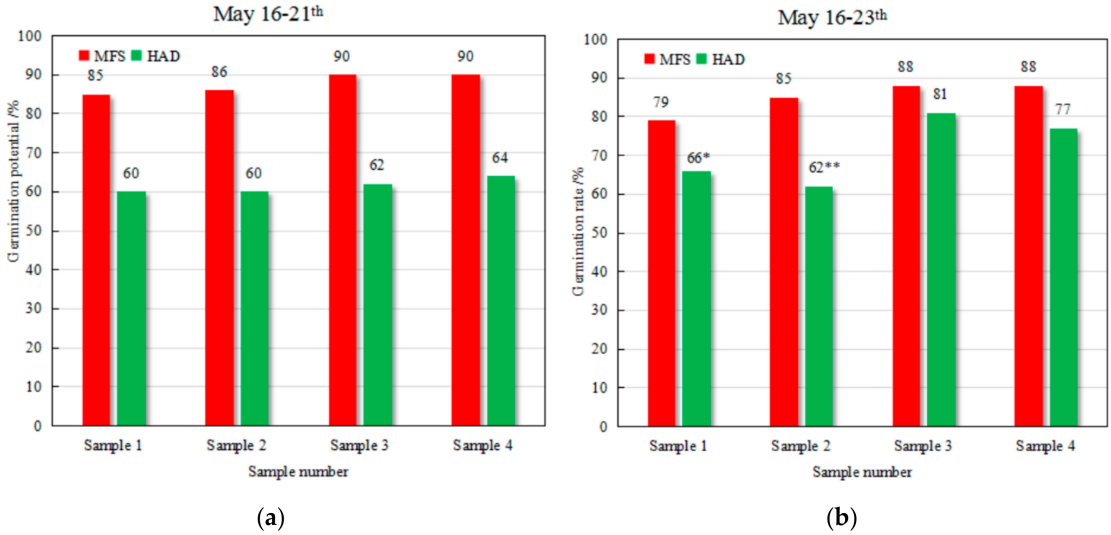

(**a**) (**b**)

Figure 5. The comparison of the germination potential (**a**) and the germination rate (**b**) of the paddy seeds. Note: * presents mild mildew, ** presents severe mildew.

Figure 6. The dried paddy seed.

As can be seen from Figure 4, the whole drying process lasts for nine hours, and the drying capacity of the dryer were ascertained to be 3.45 t/h. The industrial multi-field drying of paddy process experiences four periods including period I: Warming up period (0–60 min). In this drying period, since the evaporated water in this period can be regarded as free water and the dehydration characteristic can be summarized as free water evaporation, the moisture is quickly removed from the paddy seeds. The maximum drying rate (DR_{max} = 3.84$g_{water}/g_{dry\ matter\ hour}$) was also found at the first 60 min in the period. Period II: Falling period. In this period, since the form of water in the material is mainly expressed as bound water, more energy is needed for overcoming the binding energy between the moisture molecules and the adsorption site and less energy is used for evaporation the water [39], therefore, the drying rate in this period decreases from 3.84 $g_{water}/g_{dry\ matter\ hour}$ to 0.22 $g_{water}/g_{dry\ matter\ hour}$. Different with many other studies, there comes a constant period III between the two falling periods, which may result from the dryer construction or the drying conditions. In the last stage of the drying operation(after 390 min), the paddy temperature increases briefly due to the increased binding energy in the low moisture content of the material, the energy the paddy seed obtained is used for increasing the internal energy of the seeds and the paddy temperature is increased. Similar findings have been reported by Yang Huiping in 2012 [40]. In terms of the evaporated water, as can be seen from the Figure 4, the dehydrated water in period I, II, III, and IV are 130.75, 190.04, 60.17, and 27.39 kg and respectively account for 33.2%, 48.3%, 15.3%, and 6.9% of the total dehydrated water.

The generation rate is one of the most important indices to study the freshness of the paddy while generation potential is one of the factors for calculating seeding amount [40]. When the germination rate is the same, the seeds with high germination potential have strong vitality, which may grow better in the field. The *GP* and *GR* of the paddy seeds dried by the present dryer and general hot air dryer were investigated in a germinating bed which was sterilized by water boiling, the results are shown in Figure 5. In the six-day and eight-day tests, the *GP* and *GR* of the paddy seeds dried by the present dryer (MFD) ranges from 85% to 90% and 79% to 88%, respectively, while the *GP* and *GR* of the sample dried by general hot air dryer (HAD) ranges from 60% to 64% and 62% to 81%, respectively. Obviously, the *GR* and *GP* of the paddy seeds dried by the multi-field dryer is higher than that in the general hot air dryer, which is due to the regulating effect of far infrared ray which improved the tissue function and drying quality of seeds. The crackle ratio of the dried seeds was investigated under the crackle light, as can be seen from Figure 6, there is only one out of 100 test paddy samples crackled, that is, the crackle ratio of the paddy seed dried by *MFD* is 1%, which indicates that the quality performance of the MFD is better than the HAD.

3.2. Energy Analysis of the Dryer

3.2.1. Energy Recovery

Waste heat recovery is an effective approach to reduce energy consumption. In the present work, four tubular radiators were adopted to recover the waste heat from flue gas, in the radiator, the waste heat is converted into radiant energy which can enhance the drying even better than the thermal energy [41]. Additionally, a proper wavelength of radiation can cause the resonance of moisture molecules in the grain, the change of energy levels and increase the internal energy of the grain, thereby strengthening the drying. The radiation wavelength (λ) and the radiant energy recovered by radiator (E_{FIR}) can be calculated followed by the Equation (20) and Equation (21), respectively. The calculating results are shown in Figure 7 and, as shown in Figure 7, the wavelength of the radiator ranges from 7.89 μm to 8.15 μm. In 2003, Zhu and Zhang reported that when the far-infrared wavelength is near 9 μm, the paddy obtains the highest absorption rate of far-infrared radiation [42]. Additionally, the variation of recovered energy with drying time is shown in the figure. As can be seen from the figure, the recovered radiant energy rate in different drying time varies from 7.16 kW to 7.68 kW, and the total recovered radiant energy is 237,642.19 kJ which could evaporate almost 7.41 kg water from the wet paddy grains. Overall, the radiators can not only recover the waste heat, but also improve the quality of the product (as shown by the analysis in Section 3.1).

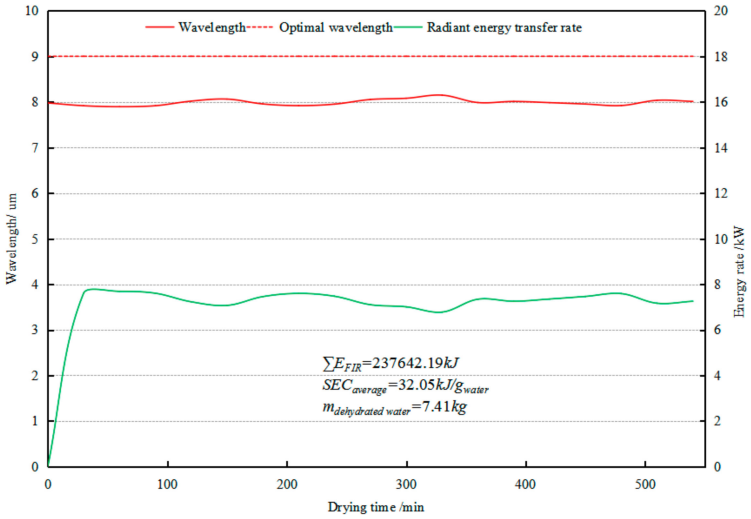

Figure 7. The wavelength of the radiator and the energy recover process.

3.2.2. Heat Loss Characteristics

To minimize the energy consumption and increase the energy efficiency of the system, heat loss characteristics of the drying chamber were investigated. In the present work, the energy loss of the drying system are mainly consisted of three parts: heat loss to surroundings(Q_{wall}), heat loss in outlet air (Q_{air}) and heat loss in outlet paddy seeds (Q_{paddy}), which can be calculated followed by Equations (15a)–15(c), respectively. The results are shown in the Figure 8. As can be seen from Figure 8, corresponding with the drying kinetics, the energy loss characteristics is divided into four period as well. In the warming up period (0–120 min), the $\dot{Q}_{wall}$, $\dot{Q}_{air}$, and $\dot{Q}_{paddy}$ briefly decreases in a small range, which is because the evaporation of water on the paddy surface takes away a lot of heat, the paddy and outlet air temperature correspondingly decreases and further leads to the decrease of the heat loss. Since the paddy temperature is lower than the outlet air temperature in the warming up period, the heat loss rate in paddy seeds is less than that in outlet air and the total heat loss for $\sum Q_{wall}$, $\sum Q_{air}$, and $\sum Q_{paddy}$ were ascertained to be 134.47, 172.76, and 73.46 MJ, respectively. Additionally, at end of the period, the drying chamber got the maximum energy efficiency of 64.28%, which indicates

that only 35.72% of the total energy input was lost at the drying time. In the first falling period, the heat loss rate in outlet air and paddy seeds increases with the increase of drying time while the heat loss rate in wall varies in a small range (32.37–36.67 kW), which may results from the almost constant inlet air temperature. In the constant period, $\dot{Q}_{wall}$, $\dot{Q}_{air}$ and $\dot{Q}_{paddy}$ varies in a very small range (31.89–34.89 kW, 77.47–87.42 kW and 120.65–124.65 kW, respectively), which may due to the impact that environment on the drying behavior. Similar with the first falling period, $\dot{Q}_{air}$ and $\dot{Q}_{paddy}$ increase with the increase of drying time in the second falling period, however, $\dot{Q}_{paddy}$ increases rapidly in this period (123.72–211.85 kW). According to some open literature [14,30,33], the binding energy between water molecule and the dry mass increases with the decrease of material moisture content, that is, under the same condition of energy input, more energy is used to increase the internal energy of the material in the low moisture content area and further leads to the increase of the paddy temperature. Thus, the heat loss in outlet paddy seeds increases rapidly, similar founding has been reported by Ma in 2012 [43]. Based on the calculation results as shown in Figure 8, the average heat loss rate was ascertained to be 468.2 MJ/h. The result is lower than the result (2036.6 MJ/h) reported by Shiun et al. for a fludilized bed dryer with drying capacity of 18 t/h [44]. Efforts should be made with respect to the insulation of the dryer body or the optimization of the inlet air temperature in the last period of the drying process.

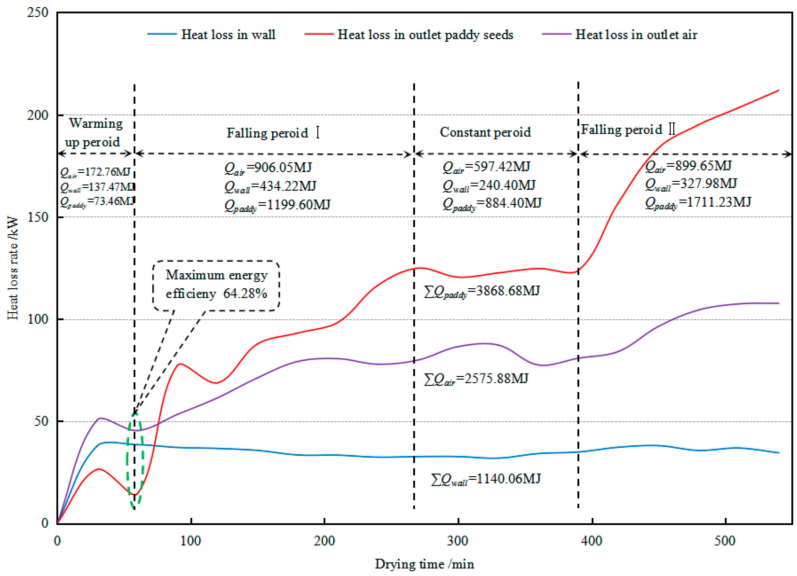

Figure 8. The heat loss characteristics of the drying chamber.

3.2.3. Energy Structure of the Drying System

Figure 9 depicts the total energy consumption ratios of the whole *MFD* system and the drying chamber, the total energy consumption of the system are mainly consisted of six aspects including the fuel, fan, negative pressure fan, conveyor, hoist and the mix, which accounts for 87.04%, 7.71%, 1.29%, 1.54%, 1.90%, and 0.51% of the total energy consumption, respectively. The fuel provides the thermal energy for air heating while the power source provided the electrical energy for the other components, the parameters of the related equipment adopted in the present work are tabulated in Table 4. In the drying chamber, the energy consumption in far-infrared drying section (*IFD*), depressurized flash drying section (*DFD*), and reverse mixed drying section (*RMD*) were investigated and the results shows that the energy consumption in *IFD*, *DFD*, and *RMD*, respectively, account for 4.87%, 1.66%, and 93.47% of the total energy consumption in the drying chamber.

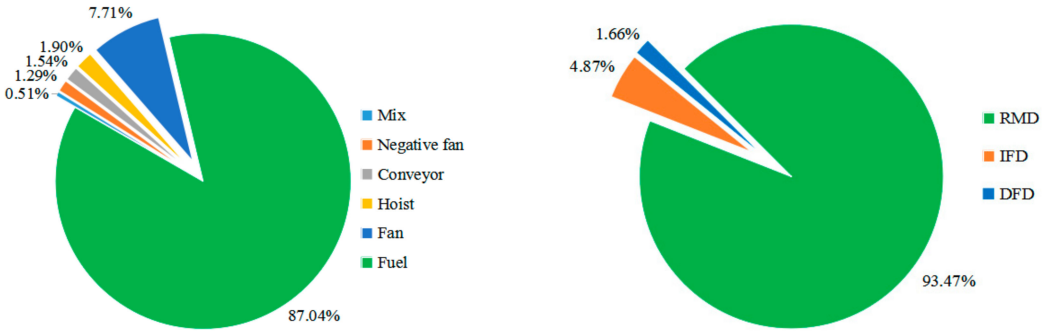

(a) **(b)**

Figure 9. Evaluation of total energy consumption of the whole drying system (**a**) and the drying chamber (**b**).

Table 4. The details of the related equipment adopted in this work.

Equipment	Power
Mix	1 kW
Hoist	3.7 kW
Conveyor	3 kW
Induced fan	15 kW
Negative pressure fan	2.5 kW

3.3. Exergy Analysis

3.3.1. Exergy Structure of the Whole System and the Drying Chamber

To increase the exergetic performance and ascertain the exergy structure of the drying chamber and the whole system during the drying process, exergy transfer rate of each component was calculated followed by Equations (6)–(14), the results are averaged and expressed as Grassmann diagram, as shown in Figure 10. For the drying chamber, the input exergy is mainly consumed by five aspects, including exergy destruction, exergy for evaporation, exergy loss to surroundings, exergy in outlet paddy seeds and air and, respectively, accounts for 55.69%, 22.25%, 10.36%, 5.7%, and 5% of the total exergy inputted into the drying chamber (18.12 kW). The average exergy loss rate in the outlet paddy seeds and outlet air are 0.91 kW and 1.03 kW, respectively. In another words, there is only 0.91 kJ and 1.03 kJ exergy loss in the outlet paddy seeds and outlet air per second, which indicates that heat exchange performance between paddy seeds and hot air flux is good. On the other hand, there are almost 22.25% of the total exergy inputted into the drying chamber is used for evaporating the moisture from the paddy grains, similar results has been reported by Sarker for rice drying in an industrial inclined bed dryer [12]. Different with the exergy structure of the drying chamber, the exergy consumed by the devices outside the drying chamber were also investigated for the exergy structure of the whole system, as can be seen from Figure 10, the exergy destruction rate gets the highest value of 23.7 kW, followed by the fan of 15 kW, water evaporation of 4.03 kW, hoist of 3.24 kW, negative pressure fan of 2.5 kW, loss to surroundings of 1.88 kW, outlet air of 1.03 kW, Mix of 1 kW, outlet paddy seeds of 0.91 kW and conveyor of 0.2 kW, and respectively accounting for 44.09%, 27.91%, 7.5%, 6.03%, 4.65%, 3.49%, 1.92%, 1.86%, 1.68%, and 0.37% of the total exergy input rate. Additionally, 0.26 kJ exergy is recovered by the radiators per second, though the recovered radiant exergy rate only accounts for 0.49% of the total exergy input rate (total recovered radiant energy can evaporate 7.41 kg water, as shown in Figure 7), the infrared radiation on the quality of paddy seeds cannot be ignored, as analyzed in Section 3.1.

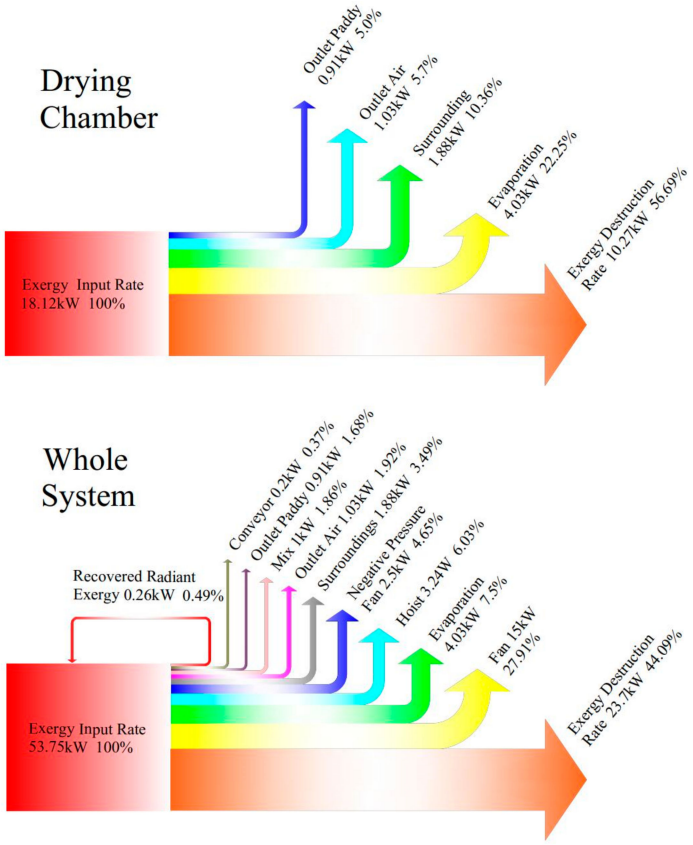

Figure 10. Grassmann diagram of the drying chamber and the whole system for the paddy seeds' multi-field drying process.

3.3.2. Exergetic Performance of the Whole System and the Drying Chamber

In the present work, the exergetic performance was investigated by applying the performance indicators including exergy efficiency (η_{ex}), improvement potential rate ($\dot{IP}$), specific energy consumption (*SEC*), and sustainability index (*SI*), which can be calculated by Equations (24)–(28), respectively. Generally, the system performance is increased by increasing the exergy efficiency, $\dot{IP}$ is used to make feasible betterment in each component throughout the whole system [45], *SEC* is used to evaluate the difficulty of the drying, and *SI* displays the effect of exergy efficiency change on sustainability [30]. The results of the exergetic performance indicators at different drying time are tabulated in Table 5.

As shown in the table, for the drying chamber and the whole system, η_{ex}, η_{en}, and *SI* decreases with the increase of drying time (or *SEC)* while $\dot{IP}$ increases with the increase of drying time except one time point (60 min). According to the heat loss characteristics analyzed in Figure 8, the heat loss rate in the point is lowest throughout the whole drying operation, generally the energy and exergy efficiency increase with the decrease of heat loss, therefore, η_{ex} and η_{en} obtain the maximum value in the point. Obviously can be seen from the table, after 390 min, *SEC* increases rapidly (35.64–99.41 kJ/g_{water}) due to the existence of the binding energy, as mentioned in Section 3.2.2. Perhaps the variable temperature drying technology (final temperature is 35.5 °C) can help to solve the problem as reported by Xiong et al. [46]. Comparing with the drying chamber at the same time, the η_{ex}, η_{en}, and *SI* correspondingly obtained lower values while $\dot{IP}$ obtained the higher value for the whole system. Of which the improvement potential rates of the drying process varies from the lowest 2.88 kW to the highest 10.59 kW for the drying chamber (accounting for 15.89–58.44% of the total exergy inputted into the drying chamber), indicating that the drying chamber has a high potential to improve the

exergy performance. While the improvement potential of the whole system varies from the lowest, 8.49 kW, to the highest, 15.83 kW, and respectively accounts for 15.81–29.48% of the total exergy input, and the results are close to the results (improvement potential accounts for 13.28–33.07% of the total exergy input) reported by Aghbaslo et al. in 2012 for fluidized bed drying of fish oil [47]. Additionally, in the present work, η_{ex} is slightly higher than η_{en} under the same drying time for both the drying chamber and the whole system, which may due to the poor irreversibility of the energy transfer process. Similar findings have been reported by Sarker et al. for paddy fluidized bed drying (energy efficiency varies from 5.24% to 13.92%, while exergy efficiency varies from 46.99% to 58.14%) in 2015 [12], Aghbashlo et al. for potato slices drying in a semi-industrial continuous dryer (energy efficiency varies from 15.13% to 37% while exergy efficiency varies from 57.13% to 94.05%) in 2008 [48].

Table 5. Energetic and exergetic performance indicators of the drying chamber and the whole system.

Drying Time/min	*SEC* (kJ/g_w)	Drying Chamber				Whole System			
		η_{ex} (%)	η_{en} (%)	$\dot{IP}$ (kW)	*SI* (-)	η_{ex} (%)	η_{en} (%)	$\dot{IP}$ (kW)	*SI* (-)
30	6.54	57.92	50.02	4.79	2.38	54.62	45.70	10.90	2.20
60	**4.98**	**76.31**	**64.28**	**2.88**	**4.22**	**60.23**	**56.63**	**8.49**	**2.51**
90	7.39	51.05	43.58	5.44	2.04	52.81	41.62	11.40	2.12
120	9.58	36.45	30.08	7.76	1.57	52.59	35.07	10.60	2.11
150	12.38	27.34	22.40	8.81	1.38	51.10	29.93	10.60	2.04
180	15.32	23.33	18.72	9.72	1.30	46.30	25.57	13.93	1.86
210	16.95	22.04	18.39	8.75	1.28	44.13	23.93	15.53	1.79
240	20.01	18.30	15.27	8.98	1.22	43.95	22.06	14.99	1.78
270	22.83	14.94	12.27	9.65	1.18	46.23	21.34	12.40	1.86
300	24.91	13.51	11.18	9.59	1.16	46.54	20.70	11.91	1.87
330	25.95	12.62	10.85	8.70	1.14	48.21	20.90	10.41	1.93
360	33.70	10.46	8.46	**10.59**	1.12	42.63	17.59	15.14	1.74
390	35.64	9.77	7.92	10.52	1.11	43.11	17.39	14.51	1.76
420	49.75	7.19	5.94	9.60	1.08	41.30	15.38	15.14	1.70
450	56.09	6.53	5.45	8.60	1.07	40.14	14.64	15.46	1.67
480	63.91	5.79	4.75	8.82	1.06	**39.03**	13.92	**15.83**	**1.64**
510	71.52	4.93	4.23	7.38	1.05	41.94	14.33	12.02	1.72
540	**99.41**	**3.65**	**3.28**	6.25	**1.04**	40.72	**13.26**	12.81	1.69
Average	32.05	22.34	18.73	8.16	1.47	46.42	25.00	12.89	1.89

Note: The values in bold are the maximum of minimum values of the corresponding indexes.

4. Conclusions

In present study, the dried rice quality, the energy and exergy performance of a novel industrial multi-field synergistic dryer were investigated. The main conclusions depending on the results of the present work are as follows:

- The average drying rate for the paddy drying in the present dryer was ascertained to be 1.21 $g_{water}/g_{wet\ matter}$ hour, and the drying rate decreased significantly after 390 min, an appropriate drying temperature for maintaining the drying rate with reasonable energy consumption should be further studied.
- The quality aspect of the product dried by the present dryer showed a better performance than that by the traditional industrial hot air dryer. The *GP* and *GR* of the paddy seeds dried by the present dryer ranged from 75% to 90% and 69% to 88%, respectively, the crackle ratio of the paddy seeds was 1%.
- After 390 min, the heat loss in outlet paddy seeds rapidly increased with the increase of drying time, which indicated that the energy efficiency should be improved in this period. The overall heat loss in outlet air, paddy seeds and in wall were ascertained to be 2575.88, 3868.68, and 1140.06 MJ, respectively.

- The total recovered radiant energy and radiant exergy recover rate were ascertained to be 237.64 MJ and 0.26 kW, respectively. Additionally, the wavelength varied from 7.89 μm to 8.15 μm, which are close to the optimal absorption wavelength of the paddy seeds.
- The overall energy and exergy efficiency of the paddy drying in the multi-field dryer ranged from 13.26% to 56.63% and 39.03% to 60.23%, respectively, indicating that the dryer is designed in an energy efficient manner.
- The improvement potential rates of the drying process varies from the lowest 2.88 kW to the highest 10.59 kW for the drying chamber and accounting for 15.89–58.44% of the total exergy inputted into the drying chamber, indicating that the drying chamber has a high potential to improve the exergetic performance.

The present work introduced a novel drying system which has the advantages of the three mentioned drying methods, the results showed that the comprehensive performance of the drying system is good and the drying system can be useful in other bioproduction processes. Additionally, the results would be helpful for further optimizing the drying process, recovering the waste heat and raising the energy utilization level. Further study is recommended to identify the appropriate drying temperature and air flows for faster drying of paddy to achieve better quality rice at reasonable energy consumption. Furthermore, a thermoeconomics analysis of the drying system is also recommended to improve the economic efficiency.

Author Contributions: The individual contributions of the present work are: writing—original draft preparation, methodology, investigation: B.L.; supervision, project administration: C.L.; data curation: T.L.; software: Z.Z.; formal analysis: W.O.; investigation: C.L.

Funding: This work was supported by the National Natural Science Foundation of China (no. 31671783; no. 31371871) and Science and Technology Planning Project of Guangdong Province, China (no. 2014B020207001).

Acknowledgments: The authors would like to thank to the editors and reviewers for their valuable and constructive comments.

Conflicts of Interest: The authors declare that we have no known competing financial interests or personal relationships that could have appeared to influence the work reported in this paper.

Nomenclature

c	specific heat ($J \cdot kg^{-1} \cdot K^{-1}$)
$\dot{\omega}$	humidity ratio of air (kg water vapor/kg dry air)
$\dot{m}$	mass flow rate ($kg \cdot s^{-1}$)
$\dot{E}$	energy rate (kW)
$\dot{E}x$	exergy rate (kW)
$\dot{Q}$	heat transfer rate (kW)
$\dot{P}$	power rate (kW)
$\dot{W}$	work rate (kW)
R	gas constant ($kJ \cdot kg^{-1} \cdot K^{-1}$)
A	cross-sectional area of the drying chamber (m^2)
v	velocity ($m \cdot s^{-1}$)
g	gravity acceleration ($m \cdot s^{-2}$)
h_{fg}	latent heat ($kJ \cdot kg^{-1}$)
T	Temperature (K or °C)
m	mass (kg)
m_i	initial wet weight (g)
m_d	final dry weight (g)
p_i	pressure (Pa)
d_g	paddy equivalent diameter (m)
$\dot{h}$	specific enthalpy ($kJ \cdot kg^{-1}$)

Abbreviations

DFD	depressurized flash drying section
IFD	far-infrared section
RMD	reverse mixed drying section
MFD	multi-field drying
HAD	hot air drying

Greek symbols

ϵ	emissivity
ρ	density (kg·m^3)
μ	dynamic viscosity (kg·m^{-1}·s^{-1})
γ	thermal conductivity (W·m^{-1}·K^{-1})
δ	thickness (m)
λ	wavelength (um)

Subscripts

a	air
p	paddy seeds
in	inlet
out	outlet
l	load
v	vapor
c	chamber
abs	absolute
da	dry air
∞	ambient
evap	evaporation
r	radiator

References

1. *Drying and Wetting of Building Materials and Components*; Delgado, J.M.P.Q., Ed.; Springer International Publishing: Basel, Switzerland, 2014; Volume 4. [CrossRef]
2. Mujumdar, A.S. *Handbook of Industrial Drying*, 3rd ed.; Taylor & Francis Group, CRC Press: Boca Raton, FL, USA, 2006. [CrossRef]
3. Kudra, T. Energy aspects in drying. *Dry. Technol.* **2004**, *22*, 917–932. [CrossRef]
4. Kemp, I.C. Fundamentals of Energy Analysis of Dryers. In *Modern Drying Technology—Energy Savings*; Tsotsas, E., Mujumdar, A.S., Eds.; Wiley-VCH Verlag GmbH: Weinheim, Germany, 2011; pp. 1–46. [CrossRef]
5. Sookramoon, K. Design of a Solar Tunnel Dryer Combined Heat with a Parabolic Trough for Paddy Drying. *Appl. Mech. Mater.* **2016**, *851*, 239–243. [CrossRef]
6. Taechapairoj, C.; Dhuchakallaya, I.; Soponronnarit, S.; Wetchacama, S.; Prachayawarakorn, S. Superheated steam fluidised bed paddy drying. *J. Food Eng.* **2013**, *58*, 67–73. [CrossRef]
7. Irfandy, F.; Djaeni, M. Evaluation of paddy quality dried with zeolite under medium temperature. *IOP Conf. Ser. Earth Environ. Sci.* **2018**, *102*, 012079. [CrossRef]
8. Suherman, S.; Djaeni, M.; Kumoro, A.C. Drying Kinetics of Paddy in Fluidized Bed with Immersed Heating Element. *Adv. Sci. Lett.* **2017**, *23*, 2364–2366. [CrossRef]
9. Krissadang, S. Performance Evaluation of a Solar Tunnel Dryer for Paddy Drying at Prathum Tani, Thailand. *Appl. Mech. Mater.* **2015**, 799–800. [CrossRef]
10. Rordprapat, W.; Nathakaranakule, A.; Tia, W.; Soponronnarit, S. Comparative study of fluidized bed paddy drying using hot air and superheated steam. *J. Food Eng.* **2005**, *71*, 28–36. [CrossRef]
11. Firouzi, S.; Alizadeh, M.R.; Haghtalab, D. Energy consumption and rice milling quality upon drying paddy with a newly-designed horizontal rotary dryer. *Energy* **2016**, *119*, 629–636. [CrossRef]
12. Sarker, M.S.H.; Ibrahim, M.N.; Aziz, N.A.; Punan, M.S. Energy and exergy analysis of industrial fluidized bed drying of paddy. *Energy* **2015**, *84*, 131–138. [CrossRef]
13. Sarker, M.; Ibrahim, M.N.; Ab Aziz, N.; Salleh, P.M. Energy and rice quality aspects during drying of freshly harvested paddy with industrial inclined bed dryer. *Energy Convers. Manag.* **2014**, *77*, 389–395. [CrossRef]

14. Li, C.; Ma, X.; Fang, Z.; Zhang, Y. Thermal energy structure of grain hot air drying and analytical method. *Trans. Chin. Soc. Agric. Eng.* **2014**, *30*, 220–228. [CrossRef]
15. Shen, Q.; Quek, S.Y. Microencapsulation of astaxanthin with blends of milk protein and fiber by spray drying. *J. Food Eng.* **2014**, *123*, 165–171. [CrossRef]
16. Ratti, C. Hot air and freeze-drying of high-value foods: a review. *J. Food Eng.* **2001**, *49*, 311–319. [CrossRef]
17. Beigi, M.; Tohidi, M.; Torki-Harchegani, M. Exergetic Analysis of Deep-Bed Drying of Rough Rice in a Convective Dryer. *Energy* **2017**, *140*. [CrossRef]
18. Folayan, J.A.; Osuolale, F.; Anawe, P. Data on exergy and exergy analyses of drying process of onion in a batch dryer. *Data Brief* **2018**, *21*, 1784–1793. [CrossRef] [PubMed]
19. Tohidi, M.; Sadeghi, M.; Torki-Harchegani, M. Energy and quality aspects for fixed deep bed drying of paddy. *Renew. Sustain. Energy Rev.* **2017**, *70*, 519–528. [CrossRef]
20. Liu, S.; Li, X.; Song, M.; Li, H.; Sun, Z. Experimental investigation on drying performance of an existed enclosed fixed frequency air source heat pump drying system. *Appl. Therm. Eng.* **2018**, *130*, 735–744. [CrossRef]
21. Aviara, N.A.; Onuoha, L.N.; Falola, O.E.; Igbeka, J.C. Energy and exergy analyses of native cassava starch drying in a tray dryer. *Energy* **2014**, *73*, 809–817. [CrossRef]
22. Aktaş, M.; Khanlari, A.; Amini, A.; Şevik, S. Performance analysis of heat pump and infrared–heat pump drying of grated carrot using energy-exergy methodology. *Energy Convers. Manag.* **2017**, *132*, 327–338. [CrossRef]
23. Hazervazifeh, A.; Nikbakht, A.M.; Moghaddam, P.A. Novel hybridized drying methods for processing of apple fruit: Energy conservation approach. *Energy* **2016**, *103*, 679–687. [CrossRef]
24. Li, C.; Mai, Z.; Fang, Z. Analytical study of grain moisture binding energy and hot air drying dynamics. *Trans. Chin. Soc. Agric. Eng.* **2014**, *30*, 236–242. [CrossRef]
25. Defraeye, T. Advanced computational modelling for drying processes—A review. *Appl. Energy* **2014**, *131*, 323–344. [CrossRef]
26. Akpinar, E.K.; Midilli, A.; Bicer, Y. The first and second law analyses of thermodynamic of pumpkin drying process. *J. Food Eng.* **2006**, *72*, 320–331. [CrossRef]
27. Bejan, A. *Advanced Engineering Thermodynamics*; John Wiley & Sons: New York, NY, USA, 1988. [CrossRef]
28. Khanali, M.; Aghbashlo, M.; Rafiee, S.; Jafari, A. Exergetic performance assessment of plug flow fluidised bed drying process of rough rice. *Int. J. Exergy* **2013**, *13*, 387–408. [CrossRef]
29. Dincer, I.; Sahin, A.Z. A new model for thermodynamic analysis of a drying process. *Int. J. Heat Mass Transf.* **2004**, *47*, 645–652. [CrossRef]
30. Yildirim, N.; Genc, S. Energy and exergy analysis of a milk powder production system. *Energy Convers. Manag.* **2017**, *149*, 698–705. [CrossRef]
31. Baird, J.K.; King, T.R. A wien displacement law for impact radiation. *Int. J. Impact Eng.* **1999**, *23*, 39–49. [CrossRef]
32. De Lima, J.A.S.; Santos, J. Generalized Stefan-Boltzmann law. *Int. J. Theor. Phys.* **1995**, *34*, 127–134. [CrossRef]
33. Li, C. Theoretical analysis of exergy transfer and conversion in grain drying process. *Trans. Chin. Soc. Agric. Eng.* **2018**, *34*. [CrossRef]
34. Aghbashlo, M.; Mobli, H.; Rafiee, S.; Madadlou, A. Energy and exergy analyses of the spray drying process of fish oil microencapsulation. *Biosyst. Eng.* **2012**, *111*, 229–241. [CrossRef]
35. Syahrul, S.; Hamdullahpur, F.; Dincer, I. Thermal analysis in fluidized bed drying of moist particles. *Appl. Therm. Eng.* **2002**, *22*. [CrossRef]
36. Skoneczna-Łuczków, J.; Ciesielczyk, W. Exergetic analysis for a complete node of a fluidized bed drying of poppy seeds. *Chem. Process. Eng.* **2015**, *36*. [CrossRef]
37. Li, J.; Chen, K.; Yang, M.; Ji, C. Studies of Paddy's Increased Crack Percentage and Sprouting Percentage after Being Dried in a Fixed Deep Bed. *Cereal Feed Ind.* **2001**. [CrossRef]
38. Yogendrasasidhar, D.; Setty, Y.P. Drying kinetics, exergy and energy analyses of Kodo millet grains and Fenugreek seeds using wall heated fluidized bed dryer. *Energy* **2018**. [CrossRef]
39. Yang, H.; Cai, X.; Chen, Q. Influence of two drying measure with two temperature to rice quality. *Grain Storage* **2013**, *1*, 34–38.
40. Chen, N.; Chen, M.; Fu, B.; Song, J. Far-infrared irradiation drying behavior of typical biomass briquettes. *Energy* **2017**, *121*, 726–738. [CrossRef]

41. Deng, Y.; Wang, Y.; Yue, J.; Liu, Z.; Zheng, Y.; Qian, B.; Zhong, Y.; Zhao, Y. Thermal behavior, microstructure and protein quality of squid fillets dried by far-infrared assisted heat pump drying. *Food Control* **2014**, *36*, 102–110. [CrossRef]
42. Zhu, W.; Zhang, Z. Research on characteristics of infrared absorption of grain. *Grain Storage* **2003**, *32*, 38–41.
43. Ma, X.; Fang, Z.; Li, C. Energy efficiency evaluation and experiment on grain counter-flow drying system based on exergy analysis. *Trans. Chin. Soc. Agric. Eng.* **2017**, *33*, 285–291. [CrossRef]
44. Shiun, L.J.; Haslenda, H.; Zainuddin, A.M.; Shariafah, R.A. Optimal design of a rice mill utility system with rice husk logistic network. *Ind. Eng. Chem.* **2012**, *51*, 362–373. [CrossRef]
45. Hepbasli, A. A review on energetic, exergetic and exergoeconomic aspects of geothermal district heating systems (GDHSs). *Energy Convers. Manag.* **2010**, *51*, 2041–2061. [CrossRef]
46. Xiong, S.; Sun, W.; Zhao, L.; Lu, Z.; He, X.; Mao, J.; Zhou, Q. Optimization of three-stage drying of paddy. *Food Sci.* **2017**, *38*, 274–281. (In Chinese with English abstract) [CrossRef]
47. Aghbashlo, M.; Mobli, H.; Madadlou, A.; Rafiee, S. Influence of spray dryer parameters on exergetic performance of microencapsulation processs. *Int. J. Exergy* **2012**, *111*, 229–241. [CrossRef]
48. Aghbashlo, M.; Kianmehr, M.H.; Arabhosseini, A. Energy and Exergy Analyses of Thin-Layer Drying of Potato Slices in a Semi-Industrial Continuous Band Dryer. *Dry. Technol.* **2008**, *26*, 1501–1508. [CrossRef]